

# Ultrafast Dynamics of Intersystem Crossing and Resonance Energy Transfer in Er(III)–Quinolinolate Complexes

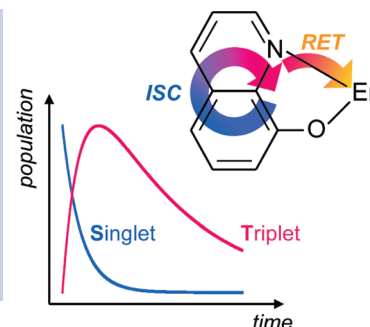
Francesco Quochi,<sup>\*,†</sup> Michele Saba,<sup>†</sup> Flavia Artizzu,<sup>‡</sup> Maria Laura Mercuri,<sup>‡</sup> Paola Deplano,<sup>‡</sup> Andrea Mura,<sup>†</sup> and Giovanni Bongiovanni<sup>†</sup>

<sup>†</sup>Dipartimento di Fisica and CGS, Università di Cagliari, SLACS-INFN/CNR I-09042 Monserrato (CA), Italy, and

<sup>‡</sup>Dipartimento di Chimica Inorganica e Analitica, Università di Cagliari, I-09042 Monserrato (CA), Italy

**ABSTRACT** Organocomplexes with trivalent erbium are investigated by time-resolved optical spectroscopy techniques. Ultrafast time scales are reported for intraligand intersystem crossing ( $\sim 10$  ps) and ligand-to-metal resonance energy transfer ( $\sim 100$  ps), resulting in lanthanide-ion sensitization with nearly unity efficiency. Given the interest of erbium complexes for telecom wavelength solid-state amplifiers and emitters, the results should stimulate further theoretical investigations on radiationless transitions in such complexes.

**SECTION** Kinetics, Spectroscopy



Lanthanide coordination complexes with organic ligands have long attracted fundamental and applied research interest owing to the possibility of sensitizing rare-earth radiative transitions at visible and near-infrared wavelengths. The promise is to achieve sensitization with high efficiency by resorting to advantageous light harvesting properties of the organic part,<sup>1</sup> that is, by designing ligands to absorb light with high efficiency in selected spectral regions. At the same time, employing lanthanide organocomplexes in films for solid-state devices would guarantee that each lanthanide ion is sensitized with the same efficiency, and quenching of lanthanide transitions due to clustering is prevented. Such complexes therefore appear suitable to solve the need for dense packing of rare earth emitters, particularly erbium, in solid-state devices, such as light-emitting diodes<sup>2</sup> and telecom optical amplifiers.<sup>3</sup> Research endeavors have concerned the determination of the lanthanide sensitization quantum yield,  $\eta_s$ , which is a key parameter for the design of functional complexes. Several relaxation steps are involved in the sensitization of the lanthanide ion, including the mixing between ligand singlet and triplet states (intersystem crossing (ISC)), which is enhanced by the “heavy-atom effect”,<sup>4</sup> and resonance energy transfer (RET) from the triplet state to the ion. In Er(III) complexes, values of  $\eta_s$  ranging from a few percents to nearly unity are inferred from available data on ion emission lifetimes and quantum yields.<sup>5–7</sup> Besides, little information has so far been collected on the intraligand and ligand-to-metal excited-state dynamics that following photoexcitation of the organic ligands leads to efficient sensitization of the Er(III) emission.<sup>8</sup>

In this work, we conduct an experimental study of the excited-state dynamics of Er(III) coordination complexes with 8-quinolinolate (Q) and partially halogenated Q derivatives as organic ligands. We excite the complexes with subpicosecond

laser pulses tuned to the fundamental intraligand absorption band and monitor the evolution of the excited-state populations with a combination of transient photoluminescence (PL) and photoinduced absorption measurements. We study the regime of linear response in which a single laser pulse creates, on average, less than one excitation per complex, and we unveil ultrafast time scales for the dynamical steps involved in Er<sup>3+</sup>-ion sensitization, namely, ISC and ligand-to-metal RET. Our finding of an unexpectedly fast ISC helps explain erbium sensitization efficiencies as high as 80 % and ion populations up to inversion threshold.<sup>7</sup> The comparison between the excited-state dynamics of Er(III)–quinolinolate complexes and those of corresponding Gd(III) and Al(III) complexes, where lanthanide sensitization is suppressed<sup>9</sup> and the heavy-atom effect is negligible, respectively, allows for discerning dynamical steps relating to erbium sensitization from other processes.

Upon near-ultraviolet photoexcitation, the organic ligands of an Er(III) complex are promoted to a singlet excited state ( $S_1$ ), which can either transfer its energy directly to a Er<sup>3+</sup> ion by RET or decay to triplet states by ISC. (See Figure 1.) RET can occur via either Dexter or Förster mechanisms, depending on total angular momentum variation ( $\Delta J$ ) undergone by the lanthanide ions.<sup>10</sup> According to information available on 8-quinolinolate and similar N-heterocycles,<sup>4</sup> the first excited singlet state  $S_1$  and the fundamental triplet state ( $T_1$ ) correspond to  $\pi-\pi^*$  transitions, whereas a triplet state involving transition from a nonbonding ( $n$ ) to a  $\pi^*$  state ( $T(n)$ ) lies in energy between  $S_1$  and  $T_1$ . Photoexcited singlets populate the

**Received Date:** July 29, 2010

**Accepted Date:** August 31, 2010

**Published on Web Date:** September 03, 2010

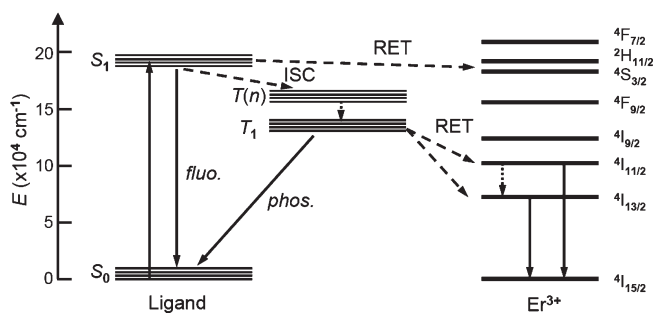


**Figure 1.** Jablonski diagram of an Er(III)–quinolinolate complex. Near-ultraviolet absorption promotes the ligand from the ground-state ( $S_0$ ) to singlet excited-state manifold ( $S_1$ ), which undergoes intersystem crossing (ISC) to intermediate triplet manifold ( $T(n)$ ) with subsequent population of the fundamental triplet manifold ( $T_1$ ). Both singlet and triplet intraligand excitons can excite the  $\text{Er}^{3+}$  ions via resonance energy transfer (RET) or decay radiatively by fluorescence (fluo.) and phosphorescence (phos.), respectively. Upon nonradiative relaxation to the first excited state ( $^4I_{13/2}$ ),  $\text{Er}^{3+}$  ions can return to their fundamental state via radiative emission at  $1.54 \mu\text{m}$  wavelength.

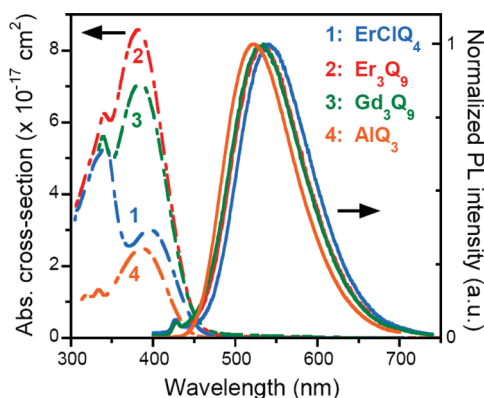


**Figure 2.** Absorption and emission spectra of metal coordination complexes with quinolinolate (Q) ligands in diluted anhydrous dimethylsulfoxide solutions. Dashed lines: Absorption cross-section spectra (left scale). Solid lines: Normalized photoluminescence (PL) spectra excited by a cw source at 380 nm wavelength (right scale).

$T(n)$  state via ISC; the  $T(n)$  intermediate state then relaxes to the  $T_1$  state. Enhancement of spin–orbit coupling due to the heavy-atom effect associated with the lanthanide ions is expected to result in acceleration of the ISC process. Efficient ISC and subsequent ligand-to-metal energy transfer by triplet excitons has so far been considered to be the main rare-earth sensitization pathway in Er(III)–quinolinolate complexes.<sup>5–8</sup>

The dynamics of the overall lanthanide sensitization process is studied on the trimetallic complex  $\text{Er}_3\text{Q}_9$  and partially halogenated, monometallic complex  $[\text{Er}(5,7\text{ClQ})_2(\text{H}5,7\text{ClQ})_2\text{Cl}]$  ( $\text{ErClQ}_4$ ).<sup>11</sup> Complementary measurements are done in Al(III) and Gd(III) complexes  $\text{AlQ}_3$  and  $\text{Gd}_3\text{Q}_9$ . The latter complex has been determined to have the same molecular structure as  $\text{Er}_3\text{Q}_9$ .<sup>12</sup> Figure 2 depicts absorption and emission spectra of all investigated complexes under cw illumination. The fundamental absorption band peaked near 400 nm, already present in the spectrum of the  $\text{Q}^-$  anion, has previously been

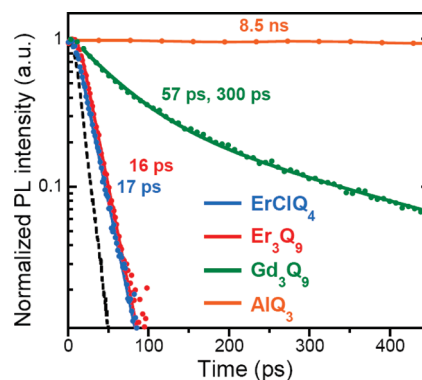


**Figure 3.** Temporal decay traces of photoluminescence (PL) intensity of metal complexes excited by subpicosecond pulses centered at 380 nm wavelength. Pulsed photoexcitation levels are set to ca.  $10^{-6}$  excited states per complex. Pulse repetition rate is 82 MHz for  $\text{ErClQ}_4$ ,  $\text{Er}_3\text{Q}_9$ , and  $\text{Gd}_3\text{Q}_9$  and 1 kHz for  $\text{AlQ}_3$ . Initial intensities are normalized to unity for ease of comparison among decay traces. Dots: Experimental data. Solid lines: Single and double exponential decay curves best fitting to experimental data. Characteristic decay times are indicated. Dashed line: Decay trace of pump light scattered by sample cuvette.

ascribed to intraligand absorption. The optical emission, spectrally peaked at ca. 550 nm, is attributed to fluorescence of singlet excitons.

Decay time of singlets critically depends on the coordinated metal ions (Figure 3): fluorescence lifetime is  $\sim 10$ – $20$  ps in  $\text{ErClQ}_4$  and  $\text{Er}_3\text{Q}_9$ ,  $\sim 60$  ps in  $\text{Gd}_3\text{Q}_9$ , for which the decay is best fitted by a double exponential function and reaches up to the 10 ns scale in  $\text{AlQ}_3$ . We do not observe triplet phosphorescence rising at longer wavelengths during fluorescence decay, implying that temporal evolution of triplets cannot be tracked by their optical emission.

Aiming at the determination of activation and decay time constants of ligand triplets, we perform transient absorption experiments with subpicosecond photoexcitation in the fundamental absorption band of the ligands. Photoinduced response of the complexes is probed in the visible (470–660 nm) and near-infrared (1400–1600 nm) regions of the optical spectrum. In addition, we measure the resonant response at the same pump (central) wavelength of 392 nm. Transient absorption  $\Delta A$  is quantified by differential transmission  $\Delta T$ , neglecting reflection, through the relation  $A = 1 - T$ , implying  $\Delta A = -\Delta T$ . The measured quantity is  $\Delta T/T = (T - T_0)/T_0$ , where  $T(T_0)$  represents the fraction of the energy of the probe pulses transmitted through the sample cuvette in presence (absence) of the pump beam.

Photoinduced absorption ( $-\Delta T/T > 0$ ) is found to dominate the response of all complexes in all spectral regions. Resonant and near-infrared signals exhibit a temporal decay that is compatible with that of the fluorescence and is thus attributed to excited-state absorption (ESA) of the  $S_1$  state (left panel of Figure 4, dynamics at infrared wavelengths is not shown). In the visible range, where activation and decay processes are observed (right panel of Figure 4), ESA is in turn ascribed to the  $T_1$  triplet state. Model curves are applied to the spectrally integrated differential transmission signals to quantify the relative contributions of singlet and triplet

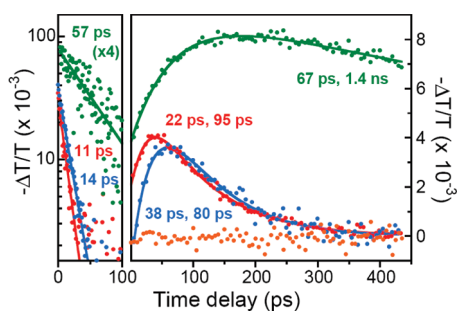


**Figure 4.** Excited-state absorption dynamics of metal complexes photopumped by subpicosecond pulses centered at 392 nm wavelength. The dynamics is reconstructed by differential transmission ( $\Delta T/T$ ) measurements versus probe-to-pump time delay. Pulsed photoexcitation levels are less than 0.2 excited states per complex. Color coding is the same as in Figures 2 and 3. Left panel: Resonant response, probed at 392 nm. Right panel: Nonresonant response probed in 570–650 nm spectral window by broadband pulses. Dots: Experimental data. Solid lines: Model curves best fitting to experimental data. (See the text for details.) Time constants of excited-state processes are indicated: singlet-decay time ( $\tau_{SD}$ ) in left panel, triplet activation ( $\tau_{TA}$ ), and decay ( $\tau_{TD}$ ) time in right panel.

ESA and to extract triplet population dynamics. Singlet and triplet ESA signals ( $S_1(t)$  and  $T_1(t)$ , respectively) are proportional to the number of excited states in the low-absorption limit and can be modeled as follows

$$S_1(t) = A_S(\lambda) \exp(-t/\tau_{SD})$$

$$T_1(t) = A_T(\lambda) \exp(-t/\tau_{TD}) \cdot [1 - \exp(t/\tau_{TD} - t/\tau_{TA})]$$

Here  $\tau_{SD}$ ,  $\tau_{TA}$ , and  $\tau_{TD}$  are the singlet-decay, triplet-activation, and triplet-decay time constants, respectively, whereas  $t$  is the time delay between pump and probe pulses;  $A_{S(T)}(\lambda)$  represents a wavelength-dependent amplitude reflecting  $S_1$  ( $T_1$ ) ESA line shape.

For each metal complex, curve fitting is conducted following a three-step procedure: (i) Singlet-decay time constant  $\tau_{SD}$  is first obtained by fitting a single exponential decay function to the resonant  $\Delta T/T$  time trace (near-infrared traces lead to the same results within 1 to 2 ps). (ii) The time trace obtained by integrating the signal over the 570–650 nm spectral window, where triplet ESA is large compared with singlet one, is fitted with the superposition function  $S_1(t) + T_1(t)$  and triplet time constants are determined. (iii) Last, the same function is applied, with  $A_{S(T)}(\lambda)$  as fitting parameters, to narrowband (20–30 nm)  $\Delta T/T$  traces with varying central wavelengths to reconstruct singlet and triplet ESA spectra. The whole procedure is justified by the fact that the decay times extracted in steps i and ii do not depend significantly on the spectral boundaries we have chosen, and singlet and triplet decay times seem constant across the spectrum.

Fit curves relating to steps i and ii are plotted as solid lines in Figure 4, whereas spectral amplitudes  $A_{S(T)}(\lambda)$  are shown in Figure 5. ESA spectra  $A_{S(T)}(\lambda)$  feature a triplet resonance peaked at ca. 525 nm in all investigated lanthanide complexes. For excited singlets, absorption decreases with increasing wavelength across the visible region and is spectrally flat in the near-infrared region. These spectra match well with

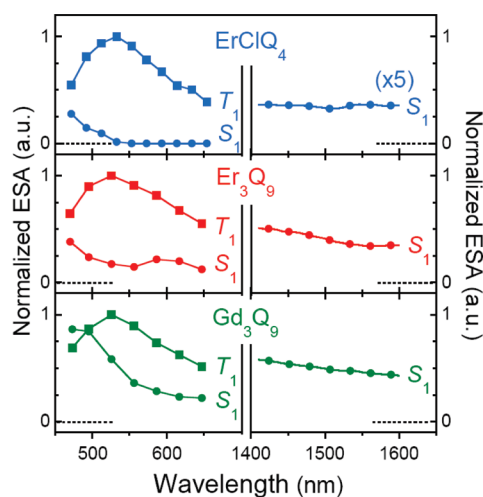


**Figure 5.** Excited-state absorption (ESA) spectra of lanthanide complexes photoexcited by ultrafast pulses centered at 392 nm wavelength and probed by broadband pulses in visible and near-infrared regions (left and right panels, respectively). Lines with dots (squares) show the reconstructed amplitudes of intraligand singlet (triplet) excited-state absorption (see text for details). Spectra are normalized to the triplet maximum at 525 nm for each complex. Dashed horizontal lines mark zero amplitude.

transient absorption ones reported in  $AlQ_3$  by Watanabe et al.,<sup>13</sup> confirming the validity of our assignment of photo-induced processes to singlet and triplet states.

It is noteworthy that curve fitting analysis yields values of the triplet activation time ( $\tau_{TA}$ ) that are systematically shorter than those of singlet decay time ( $\tau_{SD}$ ). We interpret this fact to be a result of two-step, intraligand relaxation of photoexcitations through enhanced  $S_1 \rightarrow T(n)$  ISC and subsequent  $T(n) \rightarrow T_1$  conversion. Transient population of the intermediate state  $T(n)$  appears in monometallic complex  $ErClQ_4$ , where  $S_1$  state decays in  $\sim 15$ – $20$  ps, whereas  $T_1$  state is activated in  $\sim 40$  ps.

In  $Er(III)$  complexes, inferred triplet ( $T_1$ ) decay times of  $\sim 80$ – $100$  ps show that energy transfer to the lanthanide ions is also an extremely efficient process.  $Gd_3Q_9$  acts as a control sample because the energy level spectrum of  $Gd^{3+}$  ions is empty in both visible and near-infrared regions,<sup>9</sup> so that ligand-to-metal energy transfer is suppressed; as a result, triplet decay is found to be one order of magnitude slower than that in  $Er_3Q_9$  and  $ErClQ_4$ . Parallel decay pathways such as conventional oxygen quenching can be suggested for triplets.<sup>14</sup> Being much slower than ligand-to-metal energy transfer, these processes can in fact influence only marginally lanthanide-ion sensitization efficiency in  $Er(III)$  complexes.

Efficiency of ISC ( $\eta_{ISC}$ ) in  $Er(III)$  complexes can also be evaluated by comparing triplet differential transmission amplitude, normalized to the excitation level, to the one observed in  $Gd_3Q_9$ , where  $\eta_{ISC}$  can be assumed to be unity. The comparison is carried out with the aid of curve fitting results, allowing us to estimate triplet population reached at the steady state after photoexcitation in the absence of any decay process. The results of this analysis are compatible with  $\eta_{ISC} = 1$  in both  $Er_3Q_9$  and  $ErClQ_4$ .

$AlQ_3$  is a good control compound for ISC because it presents a negligible heavy-atom effect: the determination

of a singlet lifetime of  $\sim 10$  ns in  $\text{AlQ}_3$  goes along the absence of triplet ESA in the first few hundreds of picoseconds after photoexcitation (orange dots in right panel of Figure 4).

We shall compare our findings for ISC rates with estimates based on basic rules of scale for the heavy-atom effect induced by the lanthanide ions. Spin-orbit interaction energy, responsible for singlet-triplet mixing and consequent ISC, is linearly dependent on the effective nuclear charge ( $Z$ ) of each contributing atom.<sup>4,15</sup> Neglecting all coupling terms except that with the coordinated metal (Me) ions, ISC time constant scales as  $1/Z_{\text{Me}}^2$ . Starting from a value of 100 ns for  $\text{AlQ}_3$ ,<sup>13</sup> one infers corresponding values of  $\sim 3.5$  and 4 ns for  $\text{Er}_3\text{Q}_9$  and  $\text{Gd}_3\text{Q}_9$ , respectively. The estimated values, much longer than the experimental ones (10–100 ps), hint to the necessity of a full quantum mechanical treatment of ISC rates in 8-quinolinolate lanthanide complexes.

In conclusion, we report on ultrafast ISC and ligand-to-metal RET processes in  $\text{Er(III)}$ -quinolinolate complexes investigated by transient PL and absorption spectroscopy. ISC is found to be three to four orders of magnitude faster than in  $\text{AlQ}_3$ , a phenomenon unexpected from simple rules of scale for the heavy-atom effect. Knowledge gained on lanthanide sensitization pathways in coordination complexes with organic ligands is expected to hold value for future developments with solid-state materials, for example, polymers doped with lanthanide organocomplexes featuring optical transparency in near-infrared telecom regions.<sup>16</sup>

## EXPERIMENTAL SECTION

$\text{Er(III)}$ ,  $\text{Gd(III)}$ , and  $\text{Al(III)}$  8-quinolinolate complexes are synthesized using well-established methods.<sup>11,12</sup> Complexes are dissolved in anhydrous dimethyl sulfoxide (DMSO) and loaded in quartz cuvettes for optical investigations. Absorbance spectra are recorded on  $\sim 10^{-3}$  mol  $\text{dm}^{-3}$  (M) solutions using a cw spectrophotometer. Diluted solutions ( $\sim 10^{-5}$  M) are used for fluorescence measurements in a cw spectrofluorimeter with excitation at 380 nm. For time-resolved fluorescence spectroscopy, we resort to a Ti/sapphire ultrafast oscillator delivering 100 fs long pulses with 82 MHz repetition rate. Laser pulses are frequency doubled to create an excitation beam at 380 nm central wavelength. Sample fluorescence, excited by the focused pump beam, is sent through color filters to reject laser scattered light, wavelength dispersed in a single spectrometer, and detected using a visible streak camera. Actual time resolution of the experiments is ca. 10 ps. Transient absorption experiments are performed using a Ti/sapphire regenerative amplifier delivering 150 fs pulses at 1 kHz rate. Frequency doubled pulses at 392 nm wavelength are used as the pump. Samples are optically probed in the transmission geometry using broadband pulses produced by supercontinuum generation in a sapphire plate. Probe-to-pump time delay is controlled by a motorized optical delay stage. Differential transmission is detected in visible (470–660 nm) and near-infrared (1400–1600 nm) bands using a spectrometer equipped with Si and InGaAs charge-coupled device, respectively. Signal averaging over a thousand pulses is sufficient to attain sensitivity values as low as  $2 \times 10^{-4}$  in differential transmission.

## AUTHOR INFORMATION

### Corresponding Author:

\*To whom correspondence should be addressed. Tel: +39-070-6754843. Fax: +39-070-510171. E-mail: francesco.quochi@dsf.unica.it.

**ACKNOWLEDGMENT** This work was partially funded by MIUR through FIRB projects (Synergy-FIRBRBNE03S7XZ and FIRB-RBAU01N449), by the European Commission through the Human Potential Programs (RTN Nanomatch, contract no. MRTN-CT-2006-035884), and by the Italian National Research Council (CNR) with an INFN-CNR Seed project for young researchers. F.A. thanks the Regione Autonoma della Sardegna for the cofinanced research grant funded through POR Sardegna FSE 2007-2013, L.R.7/2007 "Promozione della ricerca scientifica e dell'innovazione tecnologica in Sardegna".

## REFERENCES

- (1) See, for example: Bünzli, J.-C. G.; Piguet, C. Taking Advantage of Luminescent Lanthanide Ions. *Chem. Soc. Rev.* **2005**, *34*, 1048–1077.
- (2) Kido, J.; Okamoto, Y. Organo Lanthanide Complexes for Electroluminescent Materials. *Chem. Rev.* **2002**, *102*, 2357–2368 and references cited therein.
- (3) Kuriki, K.; Koike, Y.; Okamoto, Y. Plastic Optical Fiber Lasers and Amplifiers Containing Lanthanide Complexes. *Chem. Rev.* **2002**, *102*, 2347–2356 and references cited therein.
- (4) Lower, S. K.; El-Sayed, M. A. The Triplet State and Molecular Electronic Processes in Organic Molecules. *Chem. Rev.* **1966**, *66*, 199–241.
- (5) Comby, S.; Imbert, D.; Chauvin, A.-S.; Bünzli, J.-C. G. Stable 8-Hydroxyquinolate Podates as Efficient Sensitizers of Lanthanide Near-Infrared Luminescence. *Inorg. Chem.* **2006**, *45*, 732–743.
- (6) Albrecht, M.; Osetska, O.; Klankermayer, J.; Fröhlich, R.; Gumy, F.; Bünzli, J.-C. G. Enhancement Of Near-IR Emission By Bromine Substitution In Lanthanide Complexes With 2-Carboxamide-8-hydroxyquinoline. *Chem. Commun.* **2007**, *18*, 1854–1856.
- (7) Quochi, F.; Artizzu, F.; Saba, M.; Cordella, F.; Mercuri, M. L.; Deplano, P.; Loi, M. A.; Mura, A.; Bongiovanni, G. Population Saturation in Trivalent Erbium Sensitized by Organic Molecular Antennae. *J. Phys. Chem. Lett.* **2010**, *1*, 141–144.
- (8) Monguzzi, A.; Tubino, R.; Meinardi, F.; Biroli, A. O.; Pizzotti, M.; Demartin, F.; Quochi, F.; Cordella, F.; Loi, M. A. Novel  $\text{Er}^{3+}$  Perfluorinated Complexes for Broadband Sensitized Near Infrared Emission. *Chem. Mater.* **2009**, *21*, 128–135 and references cited therein.
- (9) Strasser, A.; Vogler, A. Phosphorescence of Gadolinium(III) Chelates under Ambient Conditions. *Inorg. Chim. Acta* **2004**, *357*, 2345–2348.
- (10) Wang, H.; Qian, G.; Wang, M.; Zhang, J.; Luo, Y. Enhanced Luminescence of an  $\text{Er(III)}$  Ion-Association Ternary Complex with a Near-Infrared Dye. *J. Phys. Chem. B* **2004**, *108*, 8084–8088 and references cited therein.
- (11) Artizzu, F.; Marchiò, L.; Mercuri, M. L.; Pilia, L.; Serpe, A.; Quochi, F.; Orrù, R.; Cordella, F.; Saba, M.; Mura, A.; et al. New Insights on Near-Infrared Emitters Based on Er-Quinolinolate Complexes: Synthesis, Characterization, Structural, and Photo-physical Properties. *Adv. Funct. Mater.* **2007**, *17*, 2365–2376.
- (12) Artizzu, F. Near-Infrared Luminescent Lanthanide Complexes of Quinolinol Ligands: Structure/Properties Relationship. Ph.D. Thesis, University of Cagliari, 2008.

- (13) Watanabe, S.; Furube, A.; Katoh, R. Generation and Decay Dynamics of Triplet Excitons in AlO<sub>3</sub> Thin Films under High-Density Excitation Conditions. *J. Phys. Chem. A* **2006**, *110*, 10173–10178.
- (14) Armelao, L.; Quici, S.; Barigelletti, F.; Accorsi, G.; Bottaro, G.; Cavazzini, M.; Tondello, E. Design of Luminescent Lanthanide Complexes: From Molecules to Highly Efficient Photo-Emitting Materials. *Coord. Chem. Rev.* **2010**, *254*, 487–505.
- (15) Beljonne, D.; Shuai, Z.; Pourtois, G.; Brédas, J. L. Spin-Orbit Coupling and Intersystem Crossing in Conjugated Polymers: A Configuration Interaction Description. *J. Phys. Chem. A* **2001**, *105*, 3899–3907.
- (16) Eldada, L.; Shacklette, L. W. Advances in Polymer Integrated Optics. *IEEE J. Sel. Top. Quantum Electron.* **2000**, *6*, 54–68.